iJRASET
International Journal For Research in
Applied Science and Engineering Technology

INTERNATIONAL JOURNAL FOR RESEARCH
IN APPLIED SCIENCE & ENGINEERING TECHNOLOGY

Volume: 14 Issue: VI Month of publication: June 2026

DOI: https://doi.org/10.22214/ijraset.2026.83723

www.ijraset.com

Call: 08813907089 | E-mail ID: ijraset@gmail.com

Spectral and Thermal Properties of Dy^{3+} ions doped Zinc Lithium Sodalime Potassiumniobate Bismuthborate Glasses

S. L. Meena
Ceramic Laboratory, Department of physics, Jai Narain Vyas University, Jodhpur 342001(Raj) India

Abstract: Glass of the system: (25-x)Bi_2O_3: 10ZnO: 10Li_2O: 10Na_2O: 10CaO: 10K_2O: 10Nb_2O_5: 15B_2O_3: xDy_2O_3. (where x=1, 1.5,2 mol %) have been prepared by melt-quenching technique. The amorphous nature of the prepared glass samples was confirmed by X-ray diffraction. DTA curve was analysed to evaluate the glass transition temperature, crystallization temperature and melting temperature.

Optical absorption and fluorescence spectra were recorded at room temperature for all glass samples. Judd-Ofelt intensity parameters Ω_λ (λ=2, 4 and 6) are evaluated from the intensities of various absorption bands of optical absorption spectra. The radiative properties like spontaneous emission probability (A), branching ratio (β), radiative life time(τ_R),stimulated emission cross–section(σ_p)and thermal properties have been evaluated.

Keywords: ZLSLPNBB Glasses, Optical Properties, Judd-Ofelt Theory, Thermal Properties.

I. INTRODUCTION

Tripositive rare earth ions have attracted much attention, because they have potential applications in many fields, such as laser action, fluorescent lamps, displays, optical devices such as frequency-conversion materials and optical fiber amplifiers [1-5].

Among different host matrices, borate glasses are quite prone with the advantages such as low non-linear refractive index, good physical, thermal and chemical stability and high transparency from near Ultra Violet to mid-Infrared region [6-10]. Borate glasses have a best thermal performance with considerable chemical durability, high gain as with low energy back transfer and weak upconversion.

They present superior properties that include high thermal expansion coefficient, high transparency, low melting point, high thermal stability and high gain density. The addition of network modifier (NWF) Li_2O is to improve both electrical and mechanical properties of such glasses. Borate glasses also exhibit high RE ions solubility [11-15].

The present work reports on the preparation and characterization of rare earth doped heavy metal oxide (HMO) glass systems for lasing materials.

I have studied on the Thermal, absorption and emission properties of Dy^{3+} doped zinc lithium sodalime potassiumniobate bismuth borate glasses. The intensities of the transitions for the rare earth ions have been estimated successfully using the Judd-Ofelt theory, The laser parameters such as radiative probabilities(A),branching ratio (β), radiative life time(τ_R) and stimulated emission cross section(σ_p) are evaluated using J.O.intensity parameters(Ω_λ, λ=2,4 and 6).

II. EXPERIMENTAL TECHNIQUES

A. Preparation of Glasses

The following Dy^{3+}doped borate glass samples (25-x)Bi_2O_3: 10ZnO: 10Li_2O: 10Na_2O: 10CaO: 10K_2O: 10Nb_2O_5:15B_2O_3:xDy_2O_3. (where x=1,1.5 and 2 mol%) have been prepared by melt-quenching method. Analytical reagent grade chemical used in the present study consist of Bi_2O_3, ZnO, Li_2O, Na_2O, CaO,K_2O,Nb_2O_5, B_2O_3 and Dy_2O_3. They were thoroughly mixed by using an agate pestle mortar. then melted at 960^{0}C by an electrical muffle furnace for 2h., After complete melting, the melts were quickly poured in to a preheated stainless steel mould and annealed at temperature of 350^{0}C for 2h to remove thermal strains and stresses. Every time fine powder of cerium oxide was used for polishing the samples. The glass samples so prepared were of good optical quality and were transparent. The chemical compositions of the glasses with the name of samples are summarized in Table 1.

International Journal for Research in Applied Science & Engineering Technology (IJRASET)
ISSN: 2321-9653; IC Value: 45.98; SJ Impact Factor: 7.538
Volume 14 Issue VI June 2026- Available at www.ijraset.com

Table 1.
Chemical composition of the glasses

Sample	Glass composition (mol %)
ZLSLPNBB (UD)	$25Bi_2O_3$: 10ZnO: $10Li_2O$: $10Na_2O$: 10CaO: $10K_2O$: $10Nb_2O_5$:$15B_2O_3$
ZLSLPNBB DY(1.0)	$24Bi_2O_3$: 10ZnO: $10Li_2O$: $10Na_2O$: 10CaO: $10K_2O$: $10Nb_2O_5$:$15B_2O_3$: 1 Dy_2O_3.
ZLSLPNBB DY(1.5)	$23.5Bi_2O_3$: 10ZnO: $10Li_2O$: $10Na_2O$: 10CaO: $10K_2O$: $10Nb_2O_5$:$15B_2O_3$:1.5 Dy_2O_3.
ZLSLPNBB DY(2.0)	$23Bi_2O_3$: 10ZnO: $10Li_2O$: $10Na_2O$: 10CaO: $10K_2O$: $10Nb_2O_5$:$15B_2O_3$:$2Dy_2O_3$.

ZLSLPNBB (UD) -Represents undoped Zinc Lithium Sodalime Potassiumniobate Bismuth Borate glass specimens.
ZLSLPNBB (DY) -Represents Dy^{3+} doped Zinc Lithium Sodalime Potassiumniobate Bismuth Borate glass specimens.

III. THEORY

A. *Oscillator Strength*

The intensity of spectral lines are expressed in terms of oscillator strengths using the relation [16].

$$f_{expt.} = 4.318 \times 10^{-9} \int \varepsilon(\nu)\, d\nu \qquad (1)$$

where, ε (*v*) is molar absorption coefficient at a given energy *v* (cm^{-1}), to be evaluated from Beer–Lambert law.
Under Gaussian Approximation, using Beer–Lambert law, the observed oscillator strengths of the absorption bands have been experimentally calculated [17], using the modified relation:

$$P_m = 4.6 \times 10^{-9} \times \frac{1}{cl} \log \frac{I_0}{I} \times \Delta\upsilon_{1/2} \qquad (2)$$

where c is the molar concentration of the absorbing ion per unit volume, I is the optical path length, $\log I_0/I$ is optical density and $\Delta\upsilon_{1/2}$ is half band width.

B. *Judd-Ofelt Intensity Parameters*

According to Judd [18] and Ofelt [19] theory, independently derived expression for the oscillator strength of the induced forced electric dipole transitions between an initial J manifold $|4f^N$ (S, L) J> level and the terminal J' manifold $|4f^N$ (S', L') J'> is given by:

$$\frac{8\Pi^2 mc\bar{\upsilon}}{3h(2J+1)}\frac{1}{n}\left[\frac{(n^2+2)^2}{9}\right] \times S(J, J') \qquad (3)$$

Where, the line strength S (J, J') is given by the equation

$$S(J, J') = e^2 \sum_{\lambda=2,4,6} \Omega_\lambda \langle 4f^N(S, L) J \| U^{(\lambda)} \| 4f^N (S', L') J' \rangle^2 \qquad (4)$$

In the above equation m is the mass of an electron, c is the velocity of light, *v* is the wave number of the transition, h is Planck's constant, n is the refractive index, J and J' are the total angular momentum of the initial and final level respectively, Ω_λ (λ=2,4and 6) are known as Judd-Ofelt intensity parameters .

C. *Radiative Properties*

The Ω_λ parameters obtained using the absorption spectral results have been used to predict radiative properties such as spontaneous emission probability (A) and radiative life time (τ_R), and laser parameters like fluorescence branching ratio (β_R) and stimulated emission cross section (σ_p).
The spontaneous emission probability from initial manifold $|4f^N$ (S', L') J'> to a final manifold $|4f^N$ (S, L) J >| is given by:

$$A[(S', L') J'; (S, L) J] = \frac{64\,\pi^2\nu^3}{3h(2J'+1)}\left[\frac{n(n^2+2)^2}{9}\right] \times S(J', \bar{J}) \qquad (5)$$

Where, $S(J', J) = e^2 [\Omega_2 \| U^{(2)} \|^2 + \Omega_4 \| U^{(4)} \|^2 + \Omega_6 \| U^{(6)} \|^2]$

The fluorescence branching ratio for the transitions originating from a specific initial manifold $|4f^N (S', L') J'\rangle$ to a final many fold $|4f^N (S, L) J\rangle$ is given by

$$\beta [(S', L') J'; (S, L) J] = \frac{A[(S' L)]}{\sum_{S L J} A[(S' L') J'(\bar{S} L)]} \qquad (6)$$

where, the sum is over all terminal manifolds.

The radiative life time is given by

$$\tau_{rad} = \sum_{S L J} A[(S', L') J'; (S,L)] = A_{Total}^{-1} \qquad (7)$$

where, the sum is over all possible terminal manifolds. The stimulated emission cross -section for a transition from an initial manifold $|4f^N (S', L') J'\rangle$ to a final manifold $|4f^N (S, L) J\rangle$ is expressed as

$$\sigma_p(\lambda_p) = \left[\frac{\lambda_p^4}{8\pi c n^2 \Delta\lambda_{eff}}\right] \times A[(S', L') J'; (\bar{S}, \bar{L})\bar{J}] \qquad (8)$$

where, λ_p the peak fluorescence wavelength of the emission band and $\Delta\lambda_{eff}$ is the effective fluorescence line width.

IV. RESULT AND DISCUSSION

A. XRD Measurement

Figure 1 presents the XRD pattern of the sample contain – B_2O_3 which is show no sharp Bragg's peak, but only a broad diffuse hump around low angle region. This is the clear indication of amorphous nature within the resolution limit of XRD instrument.

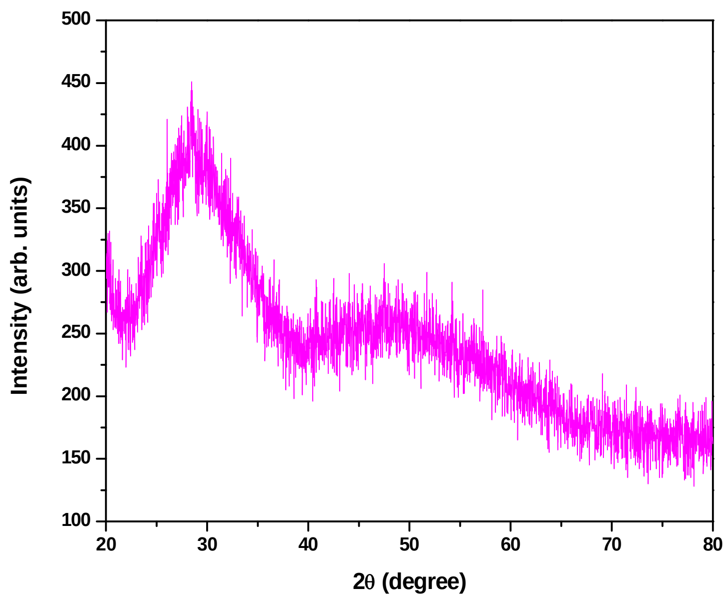

Fig. 1: X-ray diffraction pattern of ZLSLPNBB DY(1.0) glass.

B. Thermal Property

Differential thermal analysis checks the heat absorbed by glass samples during heating or cooling. Fig. 2 depicts the DTA thermogram of powdered ZLSLPNBB sample. The glass transition temperature (T_g), onset crystallization temperature (T_c), crystallization temperature (T_p), melting temperature(T_m), thermal stability (T_s),Balaji Parameter (B_P), Hurbe's criterion (H_R) and reduced glass transition temperature (T_{rg}) were calculated. Shankar's parameter also calculated by using eq. (13). All the determined thermal parameters are given in table 2.

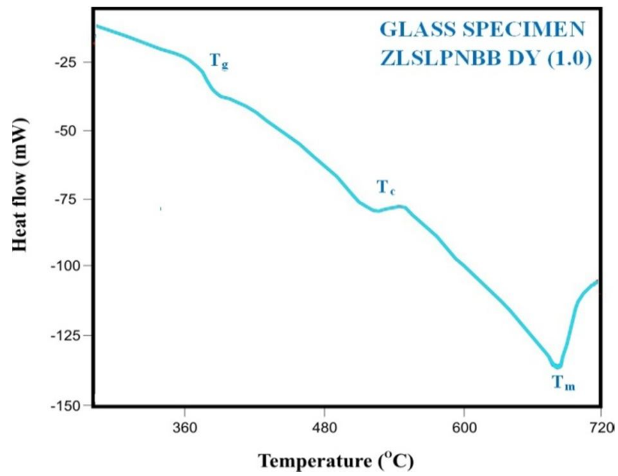

Fig.2: DTA curve of ZLSLPNBB DY (1.0) glass.

Table 2. Thermal parameters determined from the DTA traces of ZLSLPNBB DY glasses.

Sample Name	T_g (^{0}C)	T_c(^{0}C)	T_p(^{0}C)	T_m(^{0}C)	T_s(^{0}C)	B_P(^{0}C)	H_R(^{0}C)	K_S(^{0}C)	T_{rg}(^{0}C)
ZLSLPNBB DY (1.0)	375	510	548	686	134	3.436	0.220	34.574	0.547
ZLSLPNBB DY (1.5)	380	512	551	688	132	3.474	0.216	33.767	0.552
ZLSLPNBB DY (2.0)	385	514	555	693	129	3.146	0.229	32.320	0.556

The thermal stability of the glass samples can be calculated by difference between onset crystallization temperature and transition temperature [20].

Thermal Stability (T_s)= T_c-T_g (9)

Balaji Parameter can be calculated using [20].

Balaji Parameter (B_P) = $[(T_c-T_g)/(T_p-T_c)]$ (10)

Hruby's criterion is calculated using the Hurby's relation [20].

Hruby's criterion(H_R)=$[(T_p-T_c)/(T_m-T_c)]$ (11)

Reduced glass transition temperature is given as [20].

Reduced glass transition temperature (T_{rg}) =T_g/T_m (12)

Thermal Parameter is given as [20].

K_S= $[(T_m-T_c)\ (T_c-T_g)/T_m]$ (13)

C. Absorption Spectrum

The absorption spectra of ZLSLPNBB DY (1.0) glass specimen has been presented in Figure 3 in terms of Intensity versus wavelength. Thirteen absorption bands have been observed from the ground state $^6H_{15/2}$ to excited states $^6H_{13/2}$, $^6H_{11/2}$, $^6H_{9/2}$+$^6F_{11/2}$,$^6H_{7/2}$+$^6F_{9/2}$,$^6F_{7/2}$+$^6H_{5/2}$,$^6F_{5/2}$,$^6F_{3/2}$,$^6F_{9/2}$,$^4I_{15/2}$,$^4G_{11/2}$, $^6F_{7/2}$+$^4I_{13/2}$, $^6M_{19/2}$+4(P,D)$_{3/2}$ and $^4G_{9/2}$+$^6P_{3/2}$ for ZLSLPNBB DY (1.0) glass.

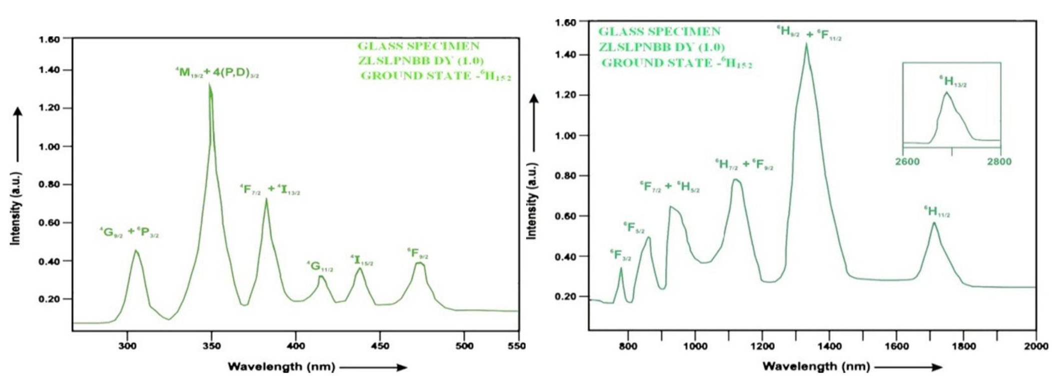

Fig. 3: Absorption spectrum of ZLSLPNBB DY(1.0) glass.

The experimental and calculated oscillator strength for Dy^{3+} ions in ZLSLPNBB glasses are given in **Table 3.**

Table 3: Measured and calculated oscillator strength ($P_m \times 10^{+6}$) of Dy^{3+}ions in ZLSLPNBB glasses.

Energy level from $^6H_{15/2}$	Glass ZLSLPNBB DY(1.0)		Glass ZLSLPNBB DY(1.5)		Glass ZLSLPNBB DY(2.0)	
	P_{exp}.	P_{cal}.	P_{exp}.	P_{cal}.	P_{exp}.	P_{cal}.
$^6H_{13/2}$	3.46	3.12	3.43	3.11	3.40	3.09
$^6H_{11/2}$	2.65	3.14	2.61	3.12	2.58	3.08
$^6H_{9/2}+^6F_{11/2}$	11.85	11.91	11.82	11.87	11.79	11.84
$^6H_{7/2}+^6F_{9/2}$	6.92	6.67	6.90	6.64	6.87	6.62
$^6F_{7/2}+^6H_{5/2}$	5.96	5.75	5.93	5.70	5.90	5.66
$^6F_{5/2}$	2.85	2.87	2.82	2.84	2.79	2.82
$^6F_{3/2}$	1.05	0.54	1.03	0.54	1.00	0.53
$^6F_{9/2}$	1.09	0.44	1.07	0.44	1.04	0.43
$^4I_{15/2}$	1.12	1.12	1.10	1.11	1.08	1.10
$^4G_{11/2}$	0.99	0.14	0.96	0.14	0.93	0.14
$^6F_{7/2}+^4I_{13/2}$	4.88	5.11	4.85	5.08	4.81	5.05
$^6M_{19/2}$+4(P,D)3/2	8.99	10.57	8.95	10.58	8.93	10.58
$^4G_{9/2}+^6P_{3/2}$	2.84	3.09	2.82	3.07	2.80	3.05
r.m.s. deviation	0.5863		0.5917		0.5892	

The values of Judd-Ofelt intensity parameters are given in Table 4.

Table 4: Judd-Ofelt intensity parameters for Dy^{3+} doped ZLSLPNBB glass specimens

Glass Specimen	$\Omega_2(pm^2)$	$\Omega_4(pm^2)$	$\Omega_6(pm^2)$	Ω_4/Ω_6	Ref.
ZLSLPNBB DY(1.0)	3.552	1.324	2.383	0.5556	P.W.
ZLSLPNBB DY(1.5)	3.531	1.337	2.358	0.5670	P.W.
ZLSLPNBB DY(2.0)	3.513	1.346	2.335	0.5764	P.W.
TB (DY)	4.910	0.630	2.290	0.2751	[21].
YZLSLMP (HO)	6.234	1.645	2.246	0.7324	[22].

D. Excitation Spectrum

The Excitation spectra of Dy^{3+}doped ZLSLPNBB glass specimens have been presented in Figure 4 in terms of Excitation Intensity versus wavelength. The excitation spectrum was recorded in the spectral region 315–465 nm fluorescence at 575nm having different excitation band centered at 321,354, 365, 385, 425, 455 and 473 nm are attributed to the $^6P_{3/2}$, $^6P_{7/2}$, $^4P_{3/2}$, $^4I_{13/2}$, $^4G_{11/2}$, $^4I_{15/2}$ and $^4F_{9/2}$ transitions, respectively. The highest absorption level is $^4I_{13/2}$ and is at 385nm.So this is to be chosen for excitation wavelength.

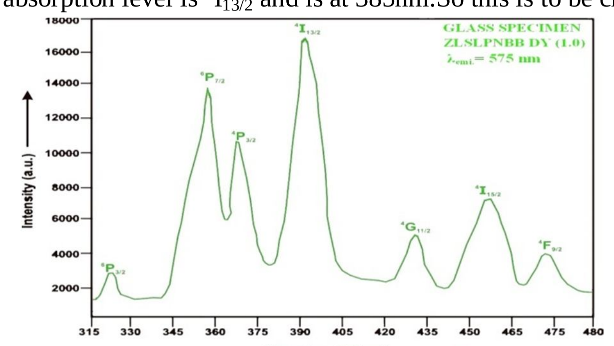

Fig. 4: Excitation spectrum of ZLSLPNBB DY(1.0) glass.

E. Fluorescence Spectrum

The fluorescence spectrum of Dy^{3+}doped in zinc lithium sodalime potassiumniobate bismuth borate glass is shown in Figure 5. There are four broad bands observed in the Fluorescence spectrum of Dy^{3+}doped zinc lithium sodalime potassiumniobate bismuth borate glass. The wavelengths of these bands along with their assignments are given in Table 5. The peak with maximum emission intensity appears at 485nm, 575 nm , 665 nm and 752 nm and corresponds to the ($^4F_{9/2}\rightarrow{}^6H_{15/2}$), ($^4F_{9/2}\rightarrow{}^6H_{13/2}$), ($^4F_{9/2}\rightarrow{}^6H_{11/2}$) and ($^4F_{9/2}\rightarrow{}^6H_{9/2}$) transition.

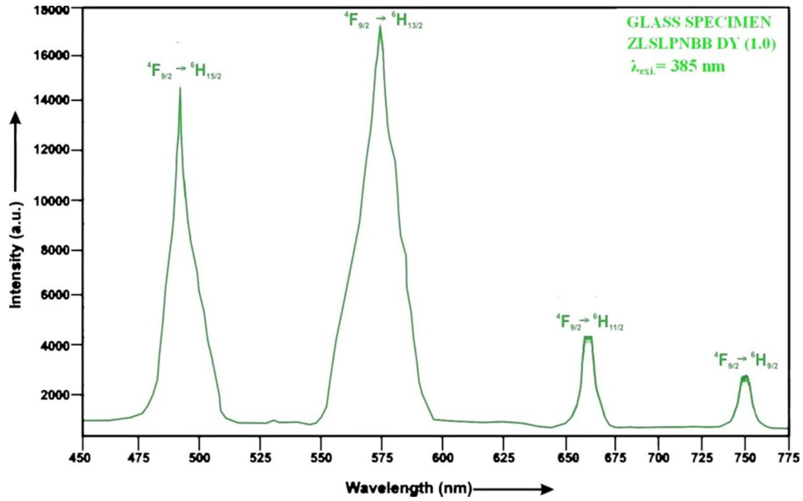

Fig. 5: Fluorescence spectrum of ZLSLPNBB DY(1.0) glass.

Table5: Emission peak wave lengths (λ_p),radiative transition probability (A_{rad}),branching ratio (β),stimulated emission cross-section(σ_p) and radiative life time(τ_R) for various transitions in Dy^{3+} doped ZLSLPNBB glasses.

Transition		ZLSLPNBB DY(1.0)				ZLSLPNBB DY(1.5)				ZLSLPNBB DY(2.0)			
	λ_{max} (nm)	$A_{rad}(s^{-1})$	β	σ_p (10^{-20} cm^2)	τ_R(μs)	$A_{rad}(s^{-1})$	β	σ_p (10^{-20} cm^2)	τ_R (μs)	$A_{rad}(s^{-1})$	β	σ_p (10^{-20} cm^2)	τ_R (10^{-20} cm^2)
$^4F_{9/2}\rightarrow{}^6H_{15/2}$	485	128.36	0.2236	0.226	1742.23	127.48	0.223	0.220	1751.04	126.66	0.2228	0.214	1759.00
$^4F_{9/2}\rightarrow{}^6H_{13/2}$	575	378.82	0.6600	1.394		377.04	0.660	1.347		375.47	0.6604	1.304	
$^4F_{9/2}\rightarrow{}^6H_{11/2}$	665	37.97	0.0662	0.168		37.83	0.0662	0.165		37.70	0.0663	0.160	
$^4F_{9/2}\rightarrow{}^6H_{9/2}$	752	28.82	0.0502	0.176		28.75	0.0503	0.174		28.68	0.0504	0.170	

V. CONCLUSION

In the present study, the glass samples of composition (25-x)Bi_2O_3: 10ZnO: 10Li_2O: 10Na_2O: 10CaO: 10K_2O: 10Nb_2O_5:15B_2O_3:xDy_2O_3. (where x =1, 1.5and 2mol %) have been prepared by melt-quenching method. The large value of Balaji and Shankar parameters indicate that the prepared glass samples have good thermal stability. The value of stimulated emission cross-section (σ_p) is found to be maximum for the transition ($^4F_{9/2}\rightarrow{}^6H_{13/2}$) for all glass specimens. This shows that ($^4F_{9/2}\rightarrow{}^6H_{13/2}$) transition is most probable transition.

REFERENCES

[1] Meena,S.L.(2025).Spectral, Thermal and Raman analysis of Ho^{3+} doped borophosphate glasses with large Balaji parameter,IOSR Appl.Phys.17,24-31.

[2] Meena, S.L.(2026).Spectral, Thermal and Raman analysis of Tm^{3+} doped in phosphate glasses for optical temperature sensor applications, IOSR Appl.Phys.18,24-30.

[3] Bondzior,B.,Lisiecki,R.(2024).Excellent Color Purity and Luminescence Thermometry Performance in Germanate Tellurite Glass Doped with Eu^{3+},Appl.Sci.14,1-15.

[4] Marzouk,M.A.,Ali,I.S.(2024).Enhancing the luminescent properties of strontium phosphate glass via controlled crystallization and rare earth dopant,35:1767,1-18.

[5] Basavapoornima,C.H.,Masthanaiah,E.,Vijay,N.,Depuru,S.R.,Kaewkhao,J.,Pecharapa,W.,Jayasankar,C.K.(2024).Spectroscopic investigation and local structure of Eu^{3+} ions in lead phosphate glasses for optical device applications,Optik,300,171667.

[6] Meena, S.L. (2025). Spectral and Thermal properties of Eu^{3+} doped Ytterium Zinc Lithium Alumina Tungsten Potassiumniobate Bismuth Borate Glasses with low Hruby's criterion, IOSR Appl.Phys.17,48-54.

[7] Prabhu,N.S.,Hegde,V.,Wagh,A.,Sayyed,M.I.,Agar,O.,Kamath,S.D.(2019).Physical,structural and optical properties of Sm^{3+} doped lithium zinc alumino borate glasses,J.Non-Cryst.Solids,515,116-124.

[8] Kilic,G.,Ilik,E.,Mahmoud,K.A.,Mallawany,R.El,Agawany,El(2020).Novel zinc vanadyl borophosphate glasses:ZnO-V_2O_5-P_2O_5-B_2O_3:Physical,thermal and nuclear radiation shielding properties,Ceram.Int.46,19318-19327.

[9] Meena,S.L.(2020),Spectroscopic Properties of Er^{3+} Doped Zinc Lithium Arsenic Strontium Vanadium Bismuth Borate Glasses, IOSR Appl.Phys.12,05-10.

[10] Meena,S.L.(2025). Spectral,Transmittance and Upconversion properties of Pr^{3+} doped bismuthborate glasses,IOSR Appl.Phys.17,20-27.

[11] Monisha, M., Nancy,A. , Souza, D., Nimitha ,V. L., Prabhu, S and Sayyed, M.I.(2020). Dy^{3+} doped SiO_2- B_2O_3-Al_2O_3-NaF-ZnF_2 glasses: An exploration of optical and gamma radiation shielding features, Current Applied Physics 20(11), 1207-1210.

[12] Kumar,S.A.,Marimuthu,K.(2013).Concentration effect of Sm^{3+} ions in B_2O_3-PbO-PbF_2-Bi_2O_3-ZnO glasses-Structural and luminescence investigations,J.Alloys Comp.565,104-114.

[13] Saisudha, M.B. and Ramakrishna J. (2002). Optical absorption of Nd^{3+}, Sm^{3+} and Dy^{3+} in bismuth borate glasses

[14] with large radiative transition probabilities. Opt. Mater. 18,403.

[15] Meena,S.L(2025).Spectral and Raman analysis of Tb^{3+} doped yttrium zinc lithium cesium barium bismuth borate glasses, IOSR,Appl.Phys.17,41-47..

[16] Zaman,F.,Rooh,G.,Srisittipokakun,N.S.,Wongdeeying,C.,Kim,H.J.,Kaewkhao,J.(2018).Physical,structural and luminescence investigation of Eu^{3+} doped lithium gadolinium bismuth borate glasses for LEDs,Solid State Sci.18,30150.

[17] Meena,S.L.(2021). Spectral and Thermal properties of Pr^{3+} doped lead lithium sodium tungsten borophosphate glasses,IOSR Appl.Phys.13,1-7.

[18] Meena,S.L.(2021). Spectral and Raman Analysis of Er^{3+} doped Zinc Lithium Antimony Sodalime Tellurite Glasses,Int.J.Eng.Sci.Inv.10,09-15.

[19] Judd, B.R. (1962). Optical Absorption Intensities of Rare Earth Ions. Physical Review, 127, 750.

[20] Ofelt, G.S. (1962). Intensities of Crystal Spectra of Rare Earth Ions. The J. Chem. Phys., 37, 511.

[21] Meena,S.L.(2026). Spectral,Thermal and Luminescent properties of Nd^{3+} doped borophosphate glasses for 1075µm NIR Photonic broad band Amplification applications, glasses, IOSR Appl.Phys.18,16-23.

[22] Boudchicha,N.,Iezid,M.,Goumeidane,F.,Legouera,M.,Prasad,P.S.,Rao,P.V.(2023).Judd-Ofelt analysis and spectroscopy study of tellurite glasses doped with rare-earth(Nd^{3+},Sm^{3+}.Dy^{3+} and Er^{3+}),Mat.16,6832,1-19.

[23] Meena,S.L.(2026).Spectral,Thermal and Photoluminescence analysis of phosphate glasses with trivalent holmium for 2.0 µm optoelectronic applications,IOSR Appl.Phys.18,01-08.